

Study on Optical Characteristics of Nano Hollow Silica with TiO₂ Shell Formation

Gi-Yeon Roh[†], Hyeong-Seok Sung, Yeong-Cheol Lee, and Seong-Eui Lee

Department of Convergence IT Device and Material Engineering, Korea Polytechnic University, Siheung 15073, Korea

(Received November 8, 2018; Revised January 8, 2019; Accepted January 9, 2019)

ABSTRACT

Optical filters to control light wavelength of displays or cameras are fabricated by multi-layer stacking process of low and high index thin films. The process of multi-layer stacking of thin films has received much attention as an optimal process for effective manufacturing in the optical filter industry. However, multi-layer processing has disadvantages of complicated thin film process, and difficulty of precise control of film morphology and material selection, all of which are critical for transmittance and coloring effect on filters. In this study, the composite TiO₂, which can be used to control of UV absorption, coated on nano hollow silica sol, was synthesized as a coating material for optical filters. Furthermore, systematic analysis of the process parameters during the chemical reaction, and of the structural properties of the coating solutions was performed using SEM, TEM, XRD and photo spectrometry. From the structural analysis, we found that the 85 nm nano hollow silica with 2.5 nm TiO₂ shell formation was successfully synthesized at proper pH control and titanium butoxide content. Photo luminescence characteristics, excited by UV irradiation, show that stable absorption of 350 nm-light, correlated with a 3.54 eV band gap, existed for the TiO₂ shell-nano hollow silica reacted with 8.8 mole titanium butoxide solution. Transmittance observed on substrate of the TiO₂ shell-nano hollow silica showed effective absorption of 200–300 nm UV light without deterioration of visible light transparency.

Key words : Nano hollow silica-titanium dioxide, Sol-gel method, Optical characteristics

1. Introduction

The structure of hollow silica nanoparticles includes a silica shell which forms the exterior and a hollow interior. Because of this structure, hollow nano silica exhibits different physical properties compared to conventional materials, and for this reason the electronic material and biochemical material industries are actively carrying out related research.¹⁾ Hollow nano silica is mainly utilized in research investigating drug delivery systems, and as a catalyst in reactions^{2,3)} as well as in display application research for refraction index control.^{4,5)}

Meanwhile, titanium dioxide particles are being studied because of their ability to decompose organic matter, act as a photocatalyst, and as a UV absorber to decrease UV transmittance.^{6,7)} The hydrothermal method, precipitation method, sol-gel method, and CVD method are used to fabricate titanium dioxide particles.⁸⁻¹¹⁾ In particular, the sol-gel method fabricates titanium dioxide through hydrolysis and heat treatment processes, which produces small sized particles which are useful for thin film coating.

Among display materials, the optical filter is used to transmit or block specific wavelengths or a wavelength range. Such optical filters can be produced through the

multi-layer thin film coating method. The multi-layer thin film coating method layers a low refractive index material and then a high refractive index material in alternating order. The properties of the film are determined by the interference of light reflected from the interface between the coating layer and the substrate.¹²⁻¹⁴⁾ However, with multi-layer thin film coating, the transmittance decreases and the wavelength blocking increases as the number of layers increases, so optimization for the application is necessary.

In this study, the high refractive index material titanium dioxide, used as a UV blocker, was applied in a shell form to the surface of hollow nano silica, which is a low refractive index material used to increase transmittance, to synthesize hollow nano silica-titanium dioxide sol to block UV. Its properties and performance for UV blocking and transmittance were analyzed.

2. Experimental Procedure

2.1. Synthesis of hollow nano silica-titanium dioxide sol according to titanium butoxide composition

Figure 1 shows a diagram of the hollow nano silica-titanium dioxide sol fabrication process. The sol-gel method was used to produce the titanium dioxide shells of the hollow nano silica particles. In order to produce the hollow nano silica-titanium dioxide sol, ethanol base hollow nano silica sol with a size of 80 nm manufactured by Vaxan Nanochem (HS-80(E), 20 wt%, Vaxan) was purchased and

[†]Corresponding author : Gi-Yeon Roh

E-mail : ngy9494@naver.com

Tel : +82-31-8041-1945 Fax : +82-31-41-1945

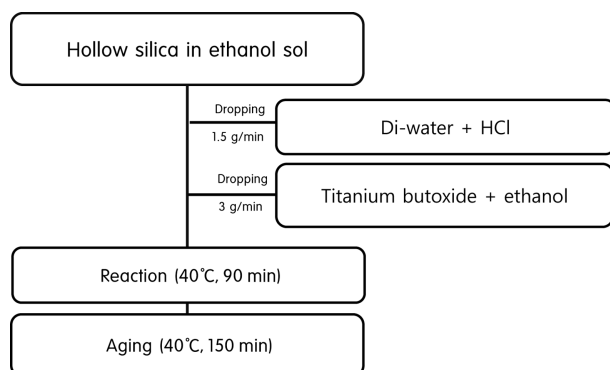


Fig. 1. Reaction flow chart of the hollow nano SiO₂-TiO₂.

used for the hollow nano silica sol solution, and titanium butoxide (TBOT) was used as the precursor of titanium dioxide. Prior to the titanium dioxide shell formation, titanium butoxide of 2.9/5.9/7.4 /8.8/14.7 mmol was added to 2.0 mol ethanol and mixed for 10 min. The hollow nano silica sol solution was diluted in ethanol to 0.1 wt% and the 0.1 wt% hollow nano silica sol solution was poured in a 3-neck reactor, mixed at 350 RPM, and heated up to 40°C. Afterwards, a metering pump was used to drop titanium butoxide and the ethanol mixture solution simultaneously at the same rate of 3 g/min, and the reaction was carried out for 90 minutes. Then, the mixture was mixed at 350 RPM and 40°C for 150 min of ageing in order to fabricate hollow nano silica-titanium dioxide according to the titanium butoxide content with a 6.68 pH.

2.2. Synthesis of hollow nano silica- titanium dioxide sol according to the change in pH

After fabricating the hollow silica-titanium dioxide sol according to the titanium butoxide content, within 1 week the formation of a precipitate was observed. In order to increase the stability of the hollow nano silica-titanium dioxide sol, a catalyst was added to control the hydrolysis and condensation reactions. To control the OH reaction on the titanium dioxide shell surface, and fabricate hollow nano silica-titanium dioxide particles, hydrochloric acid was added, which acted like a catalyst to suppress the agglomeration phenomenon between the hollow nano silica-titanium dioxide particles.^{15,16)}

Before the titanium dioxide shell formation 8.8 mmol of titanium butoxide was added to 2.0 mol of ethanol and mixed for 10 min. Also, the pH was adjusted and 0/1.4/6.9/20.6 mmol of hydrochloric acid (HCl, 20%, Daejung) was added to 50 mL of distilled water and mixed for 10 min in order to maintain the stability of the hollow nano silica-titanium dioxide sol.

The hollow nano silica sol solution was diluted in ethanol to 0.1 wt% and the 0.1 wt% hollow nano silica sol solution was poured in a 3-neck reactor to be mixed at 350 rpm and heated up to 40°C. Next, a metering pump was used to simultaneously drop the titanium butoxide and ethanol

mixture solution and the diluted hydrochloric acid solution at the same rate of 3 g/min, to carry out the reaction for 90 min. After the reaction, the mixture was mixed at 350 RPM and 40°C followed by ageing for 150 min to fabricate a hollow nano silica-titanium dioxide sol with a pH of 6.68/4.77/3.45/2.99, according to the hydrochloric acid content, with a titanium butoxide content of 8.8 mmol.

2.3. Structural and Optical Characteristics Analysis

Scanning electron microscopy (SEM, NOVA NAXO 200), transmission electron microscopy (TEM, Tecnai G2 F20S-Twin TMP), and X-ray powder diffraction (XRD, ZSX100E) were used to observe the shape and structure of the particles within the fabricated hollow nano silica-titanium dioxide sol. The optical properties of the hollow nano silica-titanium dioxide were analyzed by observations using Fluorescence Spectrometer (PL, Scinco FS-2) and a spectrophotometer (Scinco mega-800).

3. Result and Discussion

3.1. Morphology of the hollow silica-titanium dioxide based on titanium butoxide control

Figure 2 shows TEM imaging that reveals the titanium dioxide shell coating on the hollow nano silica surface, and the hollow structure produced by varying the titanium butoxide content, along with the shell thickness.

As shown in Fig. 2(a), the thickness of the hollow nano silica before the titanium dioxide shell coating was measured to be 6.3 nm. In Fig. 2(d), when the titanium butoxide content was 14.7 mmol and higher the particles with titanium dioxide shells formed as multiple particles agglomerated

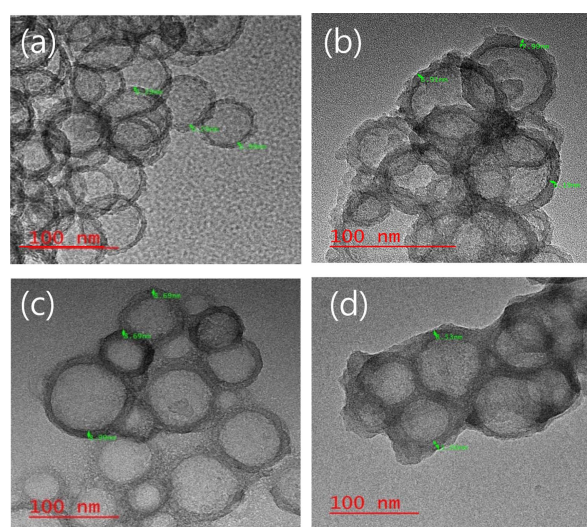


Fig. 2. TEM images of the vaxan hollow silica powders (a), and TEM images of the hollow silica-titanium dioxide particles synthesized at various concentrations of titanium butoxide: (b) 5.9 mmol (c) 8.8 mmol, (d) 14.7 mmol.

together. In Fig. 2(b), it was observed that the shell was not formed when the titanium butoxide content was insufficient, that is, when the titanium butoxide content was 5.9 mmol. The thickness of the hollow silica-titanium dioxide particle after the titanium dioxide shell coating in Fig. 2(c) was 8.69 nm, indicating a 2.5 nm titanium dioxide shell coating was present. Particles with spherical shapes and a hollow structure were formed. It was observed that when the titanium butoxide content was 8.8 mmol, the titanium dioxide shell had a completely spherical form and a shell was produced that covered the hollow silica surface.

Moreover, regardless of the titanium butoxide content, the formation of a precipitate was observed within 1 week of the hollow nano silica-titanium dioxide sol synthesis. In order to prevent the precipitation, it was necessary to maintain the sol state in the sol synthesis and storage processes by controlling the pH.

3.2. Morphology of the hollow silica-titanium dioxide based on pH control

Figure 3 shows SEM images that reveal the shape and distribution of the particles. The titanium dioxide shell was formed on the hollow nano silica surface fabricated by controlling the pH in the formation process of the hollow silica-titanium dioxide shell with a titanium butoxide content of 8.8 mmol.

Figures 3(a) and (b) show the agglomeration phenomenon that was observed after the titanium dioxide shell coating, when the pH was 6.68 and 4.77, respectively, was observed. Figs. 3(c) and (d), show that the agglomeration phenomenon gradually started at a pH of 3.45. The particle size was observed to be 85 nm.

The fabricated hollow nano silica-titanium dioxide was stored for 4 weeks to investigate its stability, and it was found that during storage no agglomeration occurred for the

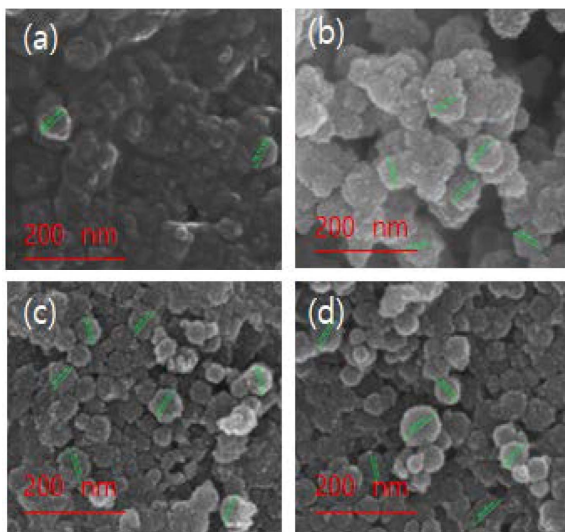


Fig. 3. SEM images of the hollow silica-titanium dioxide particles synthesized at various pH: (a) 6.68, (b) 4.77, (c) 3.45, (d) 2.99.

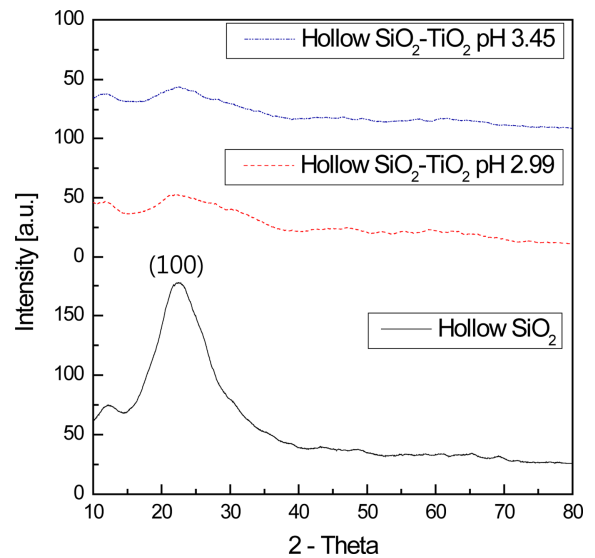


Fig. 4. XRD patterns of hollow silica and hollow silica-titanium dioxide particles synthesized at various pH: 3.45, 2.99.

samples synthesized at pH of 3.45 and 2.99.

3.3. XRD pattern analysis of the hollow silica-titanium dioxide

Figure 4 shows the XRD patterns of the hollow nano silica and hollow nano silica-titanium dioxide. For the hollow nano silica and hollow nano silica-titanium dioxide, their XRD patterns were measured after drying for 6 hours at 60°C to observe the crystal phase patterns.

In the case of the hollow nano silica, a broad pattern centered on the (100) plane was observed, indicating an amorphous state, while for the hollow nano silica-titanium dioxide, a gradual decrease in the (100) plane amorphous peak of the hollow silica was observed. A comparison of the pH of 3.45 and 2.99 samples revealed that a new amorphous peak was formed at the point corresponding to the (101) plane index of the titanium dioxide near $2\theta = 25^\circ$. This result indicates that a large amount of amorphous hollow silica and a small amount of amorphous titanium dioxide existed simultaneously.¹⁷⁻¹⁹⁾

3.4. Photoluminescence excitation spectra analysis of the hollow silica-titanium dioxide based on pH control

Figure 5 shows PL-excitation spectra according to titanium butoxide content. In the case of the hollow nano silica, sufficient excitation was not observed to occur between 300 nm–380 nm and this result was thought to be due to weak absorption in a wide wavelength range. For the hollow nano silica-titanium dioxide, a high excitation wavelength was observed at 328 nm for titanium butoxide concentrations of 2.9 mmol and 5.9 mmol. This value corresponds to 3.78 eV, which is higher than the bandgap energy of titanium dioxide, 3.2 eV. Due to the unstable amorphous structure of the

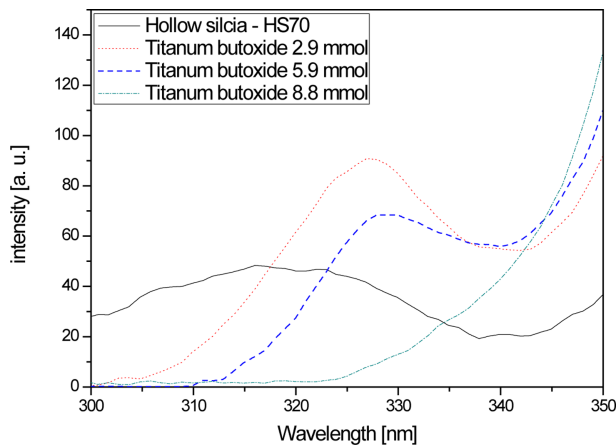


Fig. 5. PL-excitation spectra of various hollow silica and hollow silica-titanium dioxide particles synthesized at various concentrations of titanium butoxide: 2.9 mmol, 5.9 mmol, 8.8 mmol.

hollow nano silica-titanium dioxide, the energy level at which maximum absorption occurred was thought to have increased.

When the titanium butoxide content was increased to 8.8 mmol and higher, the 328 nm excitation wavelength disappeared and the excitation wavelength commonly reappeared after 350 nm. This signified that absorption was maximized at the energy level corresponding to 3.54 eV and that stable titanium dioxide shells were formed on the surfaces of the hollow nano silica particles. Hence, when the titanium butoxide composition was 5.9 mmol or lower in the synthesis process, unstable titanium dioxide shells were formed, and an unstable energy level was formed within the hollow silica bandgap, and due to this bandgap, excitation appeared to occur. For the compositions of 8.8 mmol and higher, the titanium dioxide completely coated the hollow silica surface, resulting in the disappearance of the unstable energy level, which is thought to cause the additional excitation wavelength to disappear.²⁰⁾

3.5. Optical characteristic change as coating for hollow silica-titanium thin film

Figure 6 shows the wavelength absorbance based on hollow silica-titanium dioxide thickness, after bar-coating the hollow nano silica-titanium dioxide sol, which was fabricated using a sapphire substrate with a low absorbance in thin film form that transmits both the UV range and visible light. After the bar-coating, drying was carried out for 10 minutes at 120°C and the absorbance test was conducted with the sapphire substrate as baseline and the maximum absorbance fixed to 1.0. As can be observed in Fig. 6, although it was observed that the absorption rate in the wavelength range of 200–450 nm was not high for the hollow nano silica, it was found that the absorption in the 200–350 nm range increased for the hollow nano silica-titanium dioxide film. As earlier discussed for the PL excitation result, the excitation wavelength was not observed in the

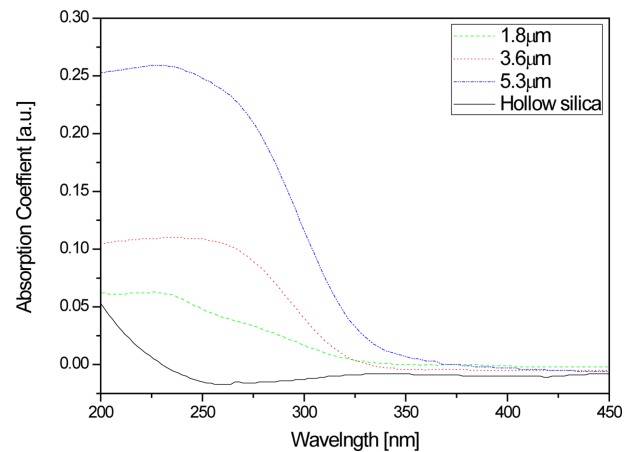


Fig. 6. Absorbance spectra of the hollow silica and absorbance spectra for different hollow SiO₂-TiO₂ thicknesses.

entire range for the hollow nano silica, and this was in agreement with the result that no light absorption occurred within the material. Meanwhile, in the case of the hollow nano silica-titanium dioxide film, absorption within the material occurred for UV of high energy wavelengths of 3.54 eV and greater, and it could be considered that the absorption of 200–350 nm light increased. Also, the absorption rate for the UV wavelength range of 200–350 nm was observed to increase as the material thickness increased. This increased light absorption was thought to be due to the increase in the thickness of the hollow nano silica-titanium dioxide particles.²¹⁾

Figure 7 shows the light transmittance of the hollow silica and hollow nano silica-titanium dioxide thin film formed on sapphire substrates.

Compared to the sapphire substrate, a decreasing trend was observed for light transmittance in the 250–350 nm wavelength range, which corresponds to UV. A transmittance of 43%, which is a 33% decrease from the 76% before

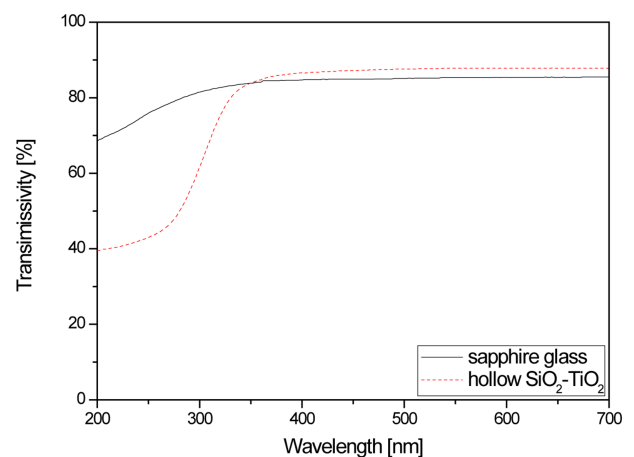


Fig. 7. Transmittance spectra of bare sapphire glass and hollow silica-titanium bar-coated sapphire glass.

the coating of the hollow nano silica-titanium dioxide, was observed at 250 nm. As discussed earlier, this result was determined to be due to a decrease in transmittance in the UV range due to the increased UV absorption of the hollow nano silica-titanium dioxide bandgap.

On the other hand, the transmittance of the sapphire substrate in the visible light range wavelength of 550 nm was 85.3% and the transmittance of the hollow nano silica-titanium dioxide was 87.8%, so the visible light transmittance increased by 2.5%. This result was thought to be due to coating the hollow nano silica-titanium dioxide sol, which removed the interference of light reflected at the interfaces of the composite between the low refractive index material silica and high refractive index material titanium dioxide.^{12–14,22)}

4. Conclusions

In this study, the refractive index was controlled to fabricate a UV blocking optical filter that minimizes the effect of light transmittance in the visible light range using a hollow nano silica sol, which enhances the light transmittance, and titanium dioxide, which is used as a UV blocker. Properties and characteristics were evaluated using equipment including SEM, TEM, XRD, photoluminescence, and spectrophotometer.

The structural properties were evaluated to confirm the formation of hollow silica-titanium dioxide particles with a size of 85 nm, and the formation of titanium dioxide shells with a thickness of 2.5 nm.

The evaluation of optical characteristics showed that when the titanium butoxide content was increased to 8.8 mmol or higher, the titanium dioxide shell formed a stable energy level with an excitation wavelength of 328 nm, corresponding to an unstable bandgap energy of 3.78 eV which appeared when the titanium butoxide content was 8.8 mmol or lower, disappeared while the excitation wavelength reappeared after 350 nm corresponding to the stable bandgap energy of 3.54 eV. With the formation of the stable bandgap, energy absorption of 3.54 eV or higher at 200–350 nm occurred when the hollow nano silica-titanium dioxide film was coated, resulting in an increase in absorbance. Also, it was observed that the transmittance in the visible light spectrum did not decrease when the coating was applied on a sapphire substrate.

These results indicate that coating a hollow nano silica-titanium dioxide sol in a thin film form and controlling the thickness can be utilized to fabricate a UV blocking optical filter that minimizes the effect of light transmittance in the visible light spectrum.

Acknowledgments

This work was supported by the Priority Research Centers Program through the National Research Foundation of Korea (NRF), funded by the Ministry of Education (NRD-2017R1A6A1A03015562).

REFERENCES

1. Z. Feng, Y. Li, D. Niu, L. Li, W. Zhao, H. Chen, J. Gao, M. Ruan, and J. Shi, "A Facile Route to Hollow Nanospheres of Mesoporous Silica with Tunable Size," *Chem. Commun.*, **23** 2629–31 (2008).
2. Z. Z. Li, L. X. Wen, L. Shao, and J. F. Chen, "Fabrication of Porous Hollow Silica Nanoparticles and Their Applications in Drug Release Control," *J. Controlled Release*, **98** [2] 245–54 (2004).
3. S. H. Wu, C. T. Tseng, Y. S. Lin, C. H. Lin, Y. Y. Hung, and C. Y. Mou, "Catalytic Nano-Rattle of Au@ Hollow Silica: Towards a Poison-Resistant Nanocatalyst," *J. Mater. Chem.*, **21** [3] 789–94 (2011).
4. Y. H. Kwak, S. C. Moon, J. S. Lee, and S. E. Lee, "A Study on the Optical Characteristics of Multi-Layer Touch Panel Structure on Sapphire Glass," *J. Korean Inst. Electr. Electron. Mater. Eng.*, **29** [3] 168–74 (2016).
5. Z. Geng and J. He, "An Effective Method to Significantly Enhance the Robustness and Adhesion-to-Substrate of High Transmittance Superamphiphobic Silica Thin Films," *J. Mater. Chem. A*, **2** [39] 16601–7 (2014).
6. D. Papoutsi, P. Lianos, P. Yianoulis, and P. Koutsoukos, "Sol-Gel Derived TiO₂ Microemulsion Gels and Coatings," *Langmuir*, **10** [6] 1684–89 (1994).
7. Y. Kotani, A. Matsuda, T. Kogure, M. Tatsumisago, and T. Minami, "Effects of Addition of Poly (Ethylene Glycol) on the Formation of Anatase Nanocrystals in SiO₂-TiO₂ Gel Films with Hot Water Treatment," *Chem. Mater.*, **13** [6] 2144–49 (2001).
8. B. M. Lee, D. Y. Shin, and S. M. Han, "Synthesis of Hydrated TiO₂ Powder by Dropping Precipitant Method and Photocatalytic Properties," *J. Korean. Ceram. Soc.*, **37** [4] 308–13 (2000).
9. C. Sanchez, J. Livage, M. Henry, and F. Babonneau, "Chemical Modification of Alkoxide Precursors," *J. Non-Cryst. Solids*, **100** [1–3] 65–76 (1988).
10. H. Y. Lee, Y. H. Park, and K. H. Ko, "Photocatalytic Characteristics of TiO₂ Films by LPMOCVD," *J. Korean Ceram. Soc.*, **36** [12] 1303–9 (1999).
11. X. Fu, W. A. Zeltner, and M. A. Anderson, "The Gas-Phase Photocatalytic Mineralization of Benzene on Porous Titania-based Catalysts," *Appl. Catal., B*, **6** [3] 209–24 (1995).
12. K. Yao, M. Koike, Y. Suzuki, K. Sakurai, T. Indo, and K. Igarashi, "Near Infrared Absorbing Film, and Multi-Layered Panel Comprising the Film," U.S. Patent No. 6,255,031, 2001.
13. Y. Shimomoto, Y. Imamura, A. Sasano, and E. Maruyama, "Striped Optical Filters Composed of Multi-Layered TiO₂ and SiO₂ Films Deposited by RF Sputtering," *Surf. Sci.*, **86** 417–23 (1979).
14. Z. Liu, X. Zhang, T. Murakami, and A. Fujishima, "Sol-Gel SiO₂/TiO₂ Bilayer Films with Self-Cleaning and Antireflection Properties," *Sol. Energy Mater. Sol. Cells*, **92** [11] 1434–38 (2008).
15. X. Z. Ding, Z. Z. Qi, and Y. Z. He, "Effect of Hydrolysis Water on the Preparation of Nano-Crystalline Titania Powders via a Sol-Gel Process," *J. Mater. Sci. Lett.*, **14** [1] 21–2 (1995).

16. Q. Chen, Y. Qian, Z. Chen, G. Zhou, and Y. Zhang, "Preparation of TiO₂ Powders with Different Morphologies by an Oxidation-Hydrothermal Combination Method," *Mater. Lett.*, **22** [1-2] 77–80 (1995).
17. R. Nandanwar, P. Singh, and F. Z. Haque, "Synthesis and Characterization of SiO₂ Nanoparticles by Sol-Gel Process and its Degradation of Methylene Blue," *Am. Chem. Sci. J.*, **5** [1] 1–10 (2015).
18. K. Thamaphat, P. Limsuwan, and B. Ngotawornchai, "Phase Characterization of TiO₂ Powder by XRD and TEM," *Kasetsart J. (Nat. Sci.)*, **42** [5] 357-61 (2008).
19. A. Welte, C. Waldauf, C. Brabec, and P. J. Wellmann, "Application of Optical Absorbance for the Investigation of Electronic and Structural Properties of Sol-Gel Processed TiO₂ Films," *Thin Solid Films*, **516** [20] 7256–59 (2008).
20. L. Tian, B. Y. Yu, C. H. Pyun, H. L. Park, and S. I. Mho, "New Red Phosphors BaZr (BO₃)₂ and SrAl₂B₂O₇ Doped with Eu³⁺ for PDP Applications," *Solid State Commun.*, **129** [1] 43–6 (2004).
21. J. Ananpattarachai, P. Kajitvichyanukul, and S. Seraphin, "Visible Light Absorption Ability and Photocatalytic Oxidation Activity of Various Interstitial N-doped TiO₂ Prepared from Different Nitrogen Dopants," *J. Hazard. Mater.*, **168** [1] 253–61 (2009).
22. L. Miao, L. F. Su, S. Tanemura, C. A. Fisher, L. L. Zhao, Q. Liang, and G. Xu, "Cost-Effective Nanoporous SiO₂-TiO₂ Coatings on Glass Substrates with Antireflective and Self-Cleaning Properties," *Appl. Energy*, **112** 1198–205 (2013).